Electronic Supplementary Information

Power discontinuity and shift of the energy onset of a molecular de-bromination reaction induced by hot-electron tunneling

Ana Barragán [a,b,c], Roberto Robles [c], Nicolás Lorente [a,c], Lucia Vitali [a,b,c,d]

a. Donostia International Physics Center (DIPC), Paseo M Lardizabal 4, 20018 San Sebastian
b. Advanced Polymers and Materials: Physics, Chemistry and Technology, Chemistry Faculty (UPV/EHU), Paseo M Lardizabal 3, 20018 San Sebastián
c. Centro de Física de Materiales CFM/MPC (CSIC-UPV/EHU), Paseo M Lardizabal 5, 20018 San Sebastián
d. Ikerbasque Research Foundation for Science, Plaza Euskadi, 5, Bilbao 48009

ESI1. Experimental and theoretical methods

ESI1a. Sample preparation and experimental characterization. The 4′-Bromo-4-mercaptobiphenyl (Br-MBP) molecules have been deposited in ultra-high vacuum conditions (UHV) onto the Au(111) surface previously prepared by cycles of Ar+ ion sputtering and subsequent annealing. The Au(Br-MBP)$_2$ molecular structure forms spontaneously on the Au(111) surface at room temperature. After the molecular deposition, the sample was transferred in UHV into a bath cryostat at the temperature of 1K to perform scanning tunneling microscopy and spectroscopy measurements.

ESI1b. Theoretical simulation. Electronic structure calculations were performed in the framework of the density functional theory (DFT) as implemented in VASP [1,2]. We used the projector augmented-wave method [3] to treat the core electrons and we expanded the wavefunctions by means of a plane-wave basis set with an energy cutoff of 400eV. We used the PBE functional [4] to treat the exchange-correlation energy. We added the missing van der Waals interactions using the Tkatchenko-Scheffler scheme [5]. We modeled the Au (111) surface using a four-layer slab. All the atoms except the lower two Au layers were relaxed until all forces were smaller than 0.02 eV/Å. We analyzed charge transfer by performing Bader analyses [6]. We have simulated the STM images within the Tersoff-Hamann approximation [7] using the method by Bocquet et al. [8] as implemented in STMpw [9]. Although, due to the size of the unit cell most calculations were performed using a gamma-point sampling, a finer (5×3×1) grid had to be used to plot the dI/dV maps. Images of charge densities and DFT models were generated using the VESTA code [10].

ESI2. Adsorption configuration and energetics

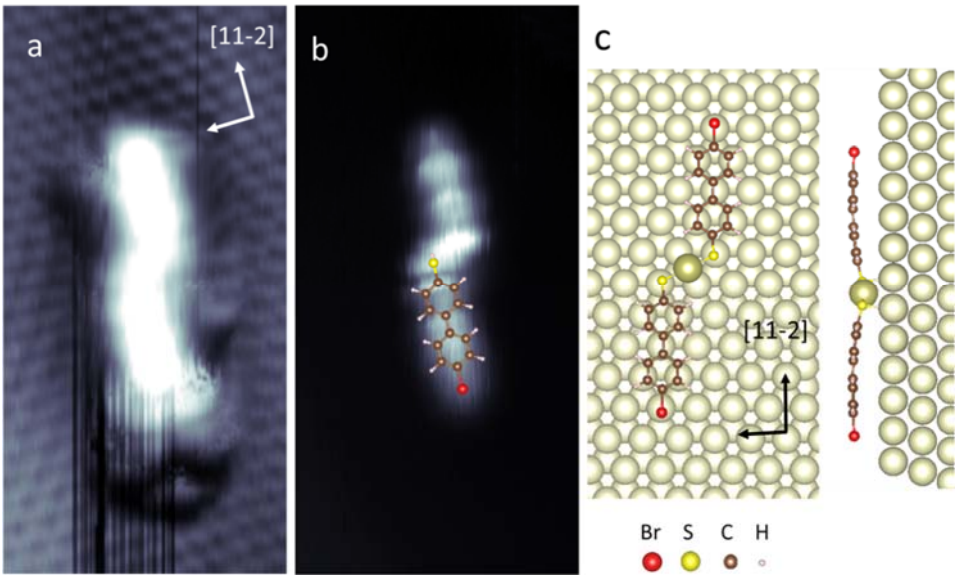

Figure ESI1. Adsorption configurations of the Au(Br-MBP)$_2$ complex on Au(111). a-b. High-resolution STM images in constant height and constant current modes, respectively, showing the molecular orientation with respect to the Au substrate high-symmetry directions and of the molecular structure (6.0nm x 3.0nm). **c.** Lowest energy DFT configuration.

Figure ESI1 shows in detail the adsorption configuration of the Au (Br-MBP)$_2$ molecular complex with respect to the Au (111) substrate directions. The sulfur atoms of the Br-MBP molecules are located on top positions of the Au (111) substrate, covalently bonded to an Au adatom, which is located in a bridge position with respect to the atomistic structure of the supporting substrate. Consequently, the molecular backbone follows the [11-2] high-symmetry direction as seen in the topographic image and in the DFT calculations configuration.

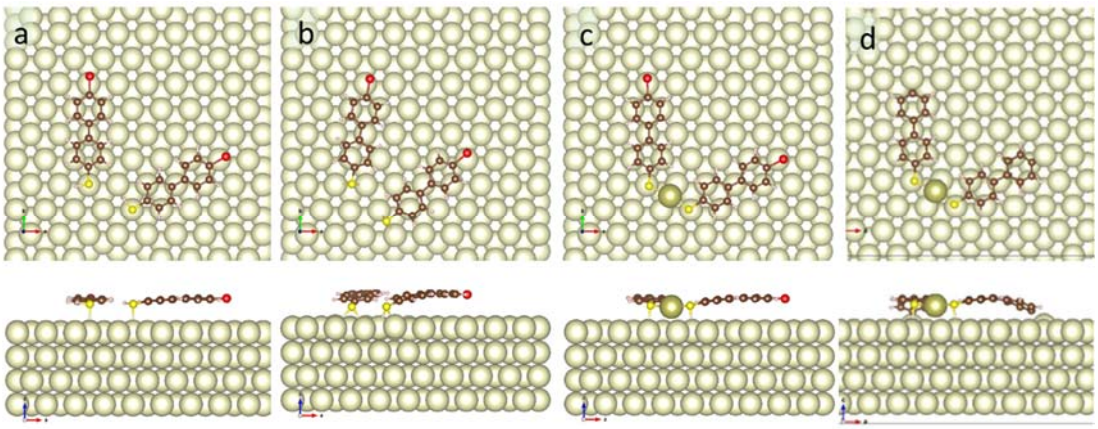

Figure ESI2. Predicted adsorption geometry (top and side views) of different configurations. a. Pristine Br-MBP molecules **b.** De-hydrogenated Br-MBP molecules. **c.** Formation of the Au (Br-MBP)$_2$ complex structure with the inclusion of an Au adatom between the S atoms. **d.** De-brominated Au (MBP)$_2$ complex.

Configuration	**Binding energy**	**Charge transfer**
a. With H, without Au adatom	$E_B = 1.92\ eV/molecule$	ΔN=-0.22e-/molecule
b. Without H, without Au adatom	$E_B = 1.58\ eV/molecule$	ΔN=0.03e-/molecule
c. Without H, with Au adatom (cis configuration) Without H, with Au adatom (trans configuration) Charge variation at S atom	$E_B = 2.30\ eV/molecule$ $E_B = 2.32\ eV/molecule$	ΔN=-0.02e-/molecule ΔN=-0.04e-/molecule ΔN=-0.05e-/atom
d. Without H and Br, with Au adatom	$E_B = 0.48\ eV/molecule$ $E'_B = 1.51\ eV/molecule$	ΔN=0.11e-/molecule

Table ESI1. Calculated adsorption energy and charge transfer (towards the substrate) by means of DFT calculations for the Au(Br-MBP)$_2$ complex self-assembled on Au(111). The different binding energies indicated in d. refer to the case in which the two halogen atoms are in gas phase or adsorbed on the surface as Br_2 specie.

Adsorption configurations calculated by DFT for different Br-MBP molecular assemblies are shown in the figure ESI2. The corresponding binding energies are summarized in the first column of the Table ESI1. The most favorable calculated structure, i.e. with higher binding energy, points that the detachment of the H atom from the –S-H termination and the bond to an Au adatom, as shown in the panel c, are energetically more stable. Upon de-bromination (panel d), the MBP molecules preserve the orientation with respect to the substrate but the adsorption is not parallel to the surface as in the Au (Br-MBP)$_2$ case shown in panel c.

In all configurations, the charge transfer of the whole molecule to the substrate is minimal, as indicated in the second column of the table ESI1. However, although the total charge transfer to Au(111) is very low, the induced charge density (left part of figure ESI3) shows that the adsorption and assembly cause a considerable rearrangement at the S-Au-S side. Thus, the induced charge and not the total charge transfer is what explains the high molecule-substrate interaction for the Au (Br-MBP)$_2$ complex. Upon de-bromination, also the -C-Au bonding at the Br side undergoes a significant change in the distribution of charges, where new bonds to the surface are formed.

ESI2a. Induced charge distribution for a pristine $Au(Br\text{-}MBP)_2$ and a de-brominated $Au(MBP)_2$ complex

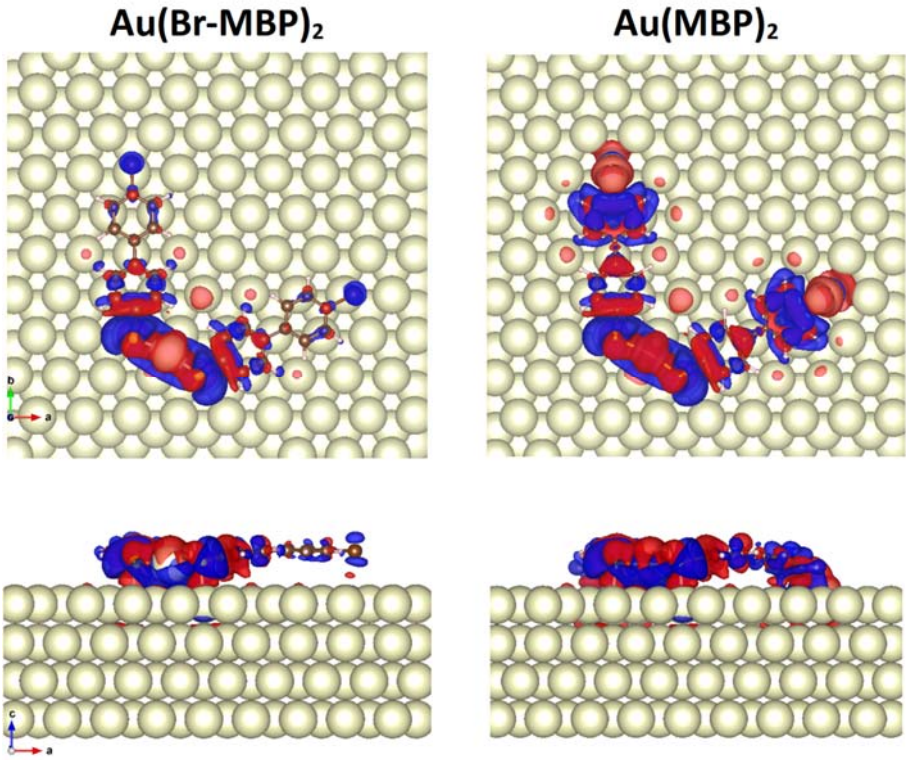

Figure ESI3. Theoretical induced charge densities for $Au(Br\text{-}MBP)_2$ and $Au(MBP)_2$ molecular structures. Blue means electron depletion, red means electron accumulation. Isovalue=0.005 electrons per Angström^3.

Figure ESI3, shows the predicted induced charge densities for the pristine $Au(Br\text{-}MBP)_2$ molecular structure, which is highly localized at the S-Au-S side. On the other hand, for the de-brominated $Au(MBP)_2$ complex, the induced charge is localized not only at the S-Au-S side but also at the new C-Au anchoring positions, as shown in the right side.

ESI3. Experimental cis (V-shaped) – trans (S-shaped) manipulation

Br-MBP molecules adsorb on Au (111) either on *cis* ("V" shaped) or on *trans* ("S-"shaped). These two configurations are energetically equivalent and can easily be inter-exchanged by manipulating one Br-MBP molecule with the tip of the microscope. Figure ESI4 shows one example of this manipulation, from a *trans* to a *cis* structure, after approaching 100 pm the tip of the STM to one of the molecules of the complex, at -10mV and 300pA. This manipulation shows that the cis-trans transformation is controlled by a low-energy barrier. However, the molecular complex cannot be displaced along the surface due to the strong interaction of the S-Au-S bond.

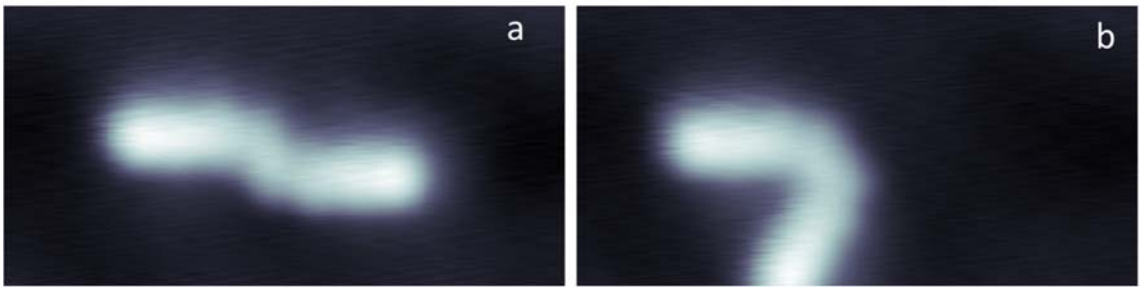

Figure ESI4. Experimental molecular manipulation.

ESI4. Projected density of states of the pristine Au (Br-MBP)$_2$ and the de-brominated Au (MBP)$_2$ complex on Au(111) surface

Figure ESI5 shows the projected density of states (PDOS) of the Au(Br-MBP)$_2$ molecular complex (black curve) and of the de-brominated Au(MBP)$_2$ complex (dashed curve). The projected density of states of Br atoms to the pristine specie is also shown in red in order to clarify its contribution.

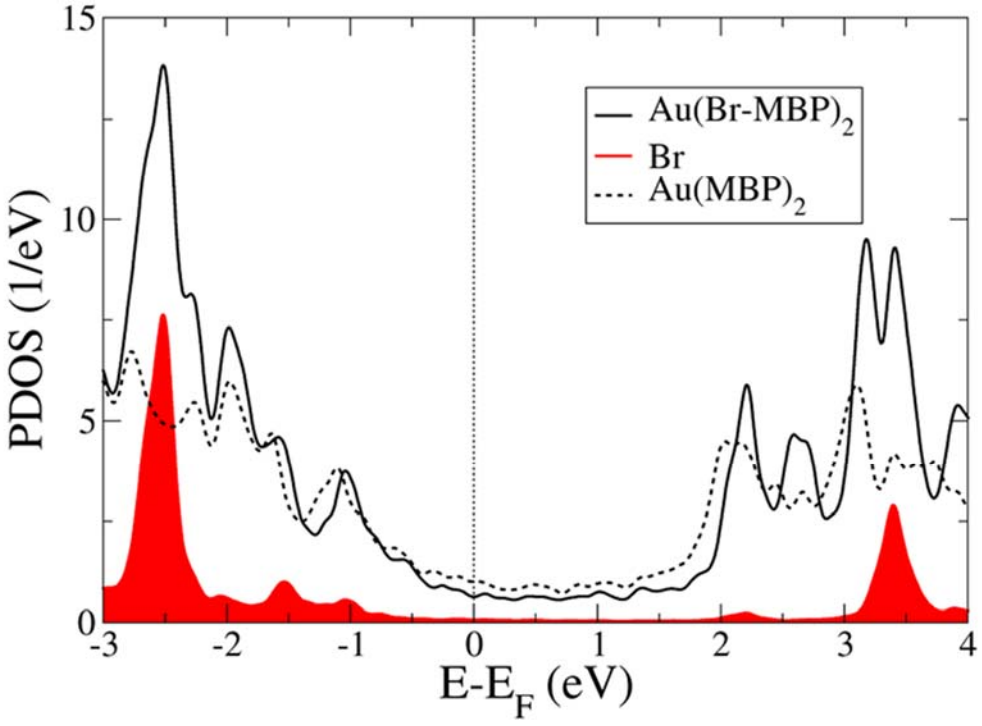

Figure ESI5. **Projected density of states (PDOS)** of pristine Au(Br-MBP)$_2$ and de-brominated Au(MBP)$_2$ molecular complex. The contribution of Br atoms to the pristine specie is shown in red.

ESI5. De-bromination dynamics and tunnel-current power into de-bromination

The de-bromination dynamics is a complex process that involves the excitation of the Br-molecule bond and its evolution. Once excited, the Br atom can evolve into dissociation or into de-excitation.

The number, *N*, of excited Br atoms that can eventually end up in a de-bromination event is given by the rate equation:

$$\frac{dN}{dt} = \gamma I N_0 - \frac{1}{\tau} N$$

where, γ is the inelastic fraction of electrons that excite the Br bond, γI is the rate of excitation of the molecule, which is linearly dependent on the applied electronic current, *I*, taking into account that more excitation events can take place at larger currents. $1/\tau$ is the rate of the de-excitation into the initial ground state of the brominated molecule.

Using detailed balance, we have that the sum of populations of excited molecules, *N*, and ground state molecules, N_0, should be 100%. In steady state, we can easily solve for the current that leads to a certain population *N* of excited molecules, given by:

$$I = \frac{\frac{1}{\tau} N}{\gamma (1 - N)}$$

Thus, the de-bromination power is easily computed using $P = IV$.

As each molecular electronic resonance constitutes a new way of exciting the molecule, the opening of a new molecular channel, implies an increase of the inelastic fraction. We understand that in our experiment the threshold and sudden change in the de-bromination power at 3.6V corresponds to the onset of a second electronic resonance of the molecule. This threshold coincides with the threshold for bulk states above the L-L' gap of Au (111), thus the strong hybridization of the molecular resonance with the bulk states of Au leads to a broad molecular resonance and renders the electron-molecule coupling very efficient.

We take into account this process by writing the inelastic fraction as the contribution of two inelastic fractions over the Au (111) bulk threshold. The final power above the bulk threshold becomes:

$$P = \frac{\frac{1}{\tau} NV}{(\gamma_1 + \gamma_2)(1 - N)}$$

Consequently, we see that the power increases linearly with bias, except when the bias crosses the threshold and the denominator suddenly increases due to the opening of a new inelastic channel. When the new channel opens, the power suddenly drops, and coincidentally the slope with bias changes as shown in Figure 3 of the main text. We underline that in order to get reasonably good agreement with the experimental data, we need to consider that about 10% of the tunneling current result into an inelastic excitation of the Br-bond which is a usual fraction in the electron tunneling for exciting molecular vibrations and a de-excitation lifetime in the range of 100 - 200 ps. Besides the large

number of parameters, we quickly realize that there are not so many options when reasonable numbers are used. In particular, we notice that long lifetimes (100 to 200 ps) of the excited Br are needed in order to efficiently de-brominate the molecule.

ESI6. De-Bromination power

Figure ESI6 focuses on the discontinuity region of the IV curve observed upon the detachment of the Br atom. The sharp and sudden change in the tunnelling current allows an easy identification of the critical current and voltage occurring upon a debromination event.

Specifically, the crossing point of the black dashed-lines corresponds to the critical value at which the dehalogenation takes place. This value is used to calculate the power for each of the events shown in figure 3 of the main text. Due to the sharpness of the discontinuity, $V_{de\text{-}Br}$ and $I_{de\text{-}Br}$ can be determined easily and unequivocally. The grey lines provides a rough idea of how the selection of a neighbouring point shifted of few pA in the IV curve would lead to a not correct estimate of the debromination voltage. Even so, the average between the two selections (black and grey) would be 3.142±0.005V and 6.09±0.04nW, respectively. Thus, the measurements uncertainties are too small to influence the conclusions of the work minimally and to be observed in figure 3 of the main text.

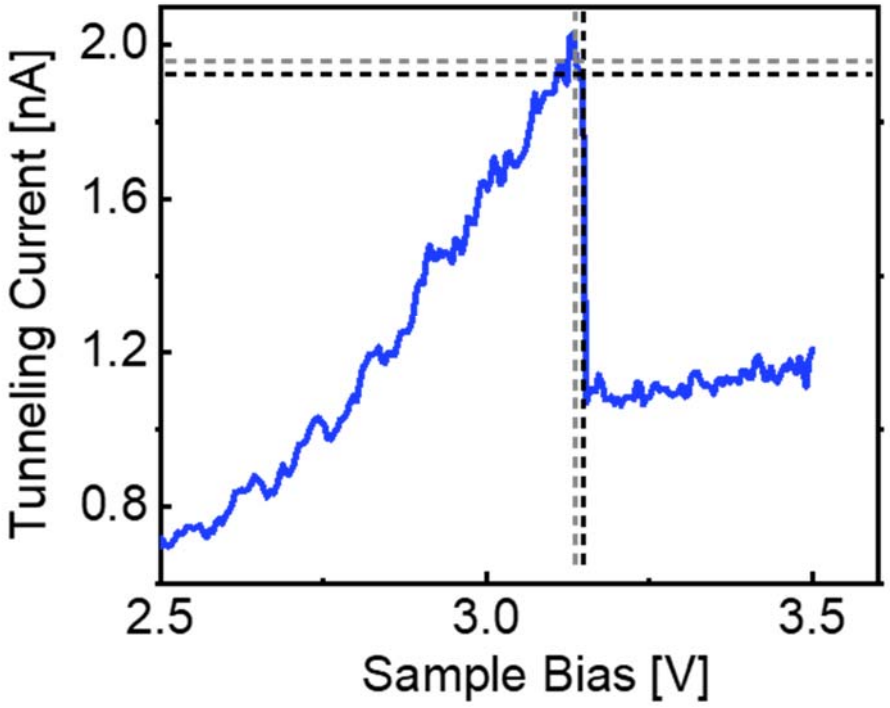

Figure ESI6. Estimate of power during debromination. Zoom in the discontinuity region of the IV curve shown in figure 3f . Black and grey dashed lines indicate two possible different choices in the measurements of the dehalogenation conditions. The crossing point of the black lines is used to determine the $I_{de\text{-}Br}$ and $V_{de\text{-}Br}$ for graph 3 of main text.

ESI7. Bulk states onset on Au (111)

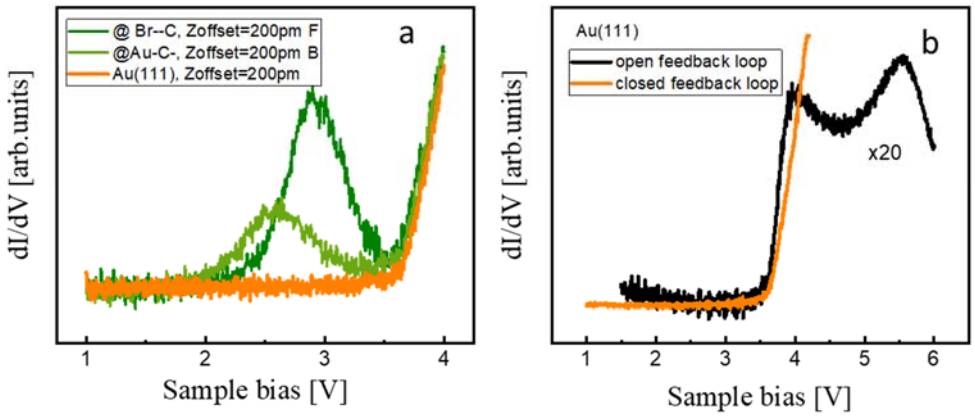

Figure ESI7. Comparison of DOS measured on different sites. a. dI/dV spectra measured on the Au(Br-MBP)$_2$ pristine and de-brominated structures (green curves, also shown in figure 3 of the main manuscript) compared with the one measured on the clean Au(111) (orange curve). **b.** Comparison of dI/dV spectra measured on Au (111) with closed (orange) and open (black) feedback loop

Figure ESI7 shows the experimental dI/dV spectra measured on top of the Br atom of a pristine Au(Br-MBP)$_2$ and a de-brominated Au(MBP)$_2$ molecular complex (pristine: green curve showing the characteristic peak at 2.9V, de-brominated: light- green curve with peak at an energy around 2.5V). These spectra are compared with the dI/dV curve obtained on the clean Au(111) substrate (orange curve). The comparison of these spectra confirms that the sharp increase of the DOS at energies larger than 3.6V have origin on the Au(111). The panel b shows the steep rise in the dI/dV spectra from 3.6V is due to the onset of bulk states of Au (111). Orange and black curve are measured on the same position with closed and open feedback loop, respectively.

ESI8. Calculated equilibrium position of the dissociated Br atom

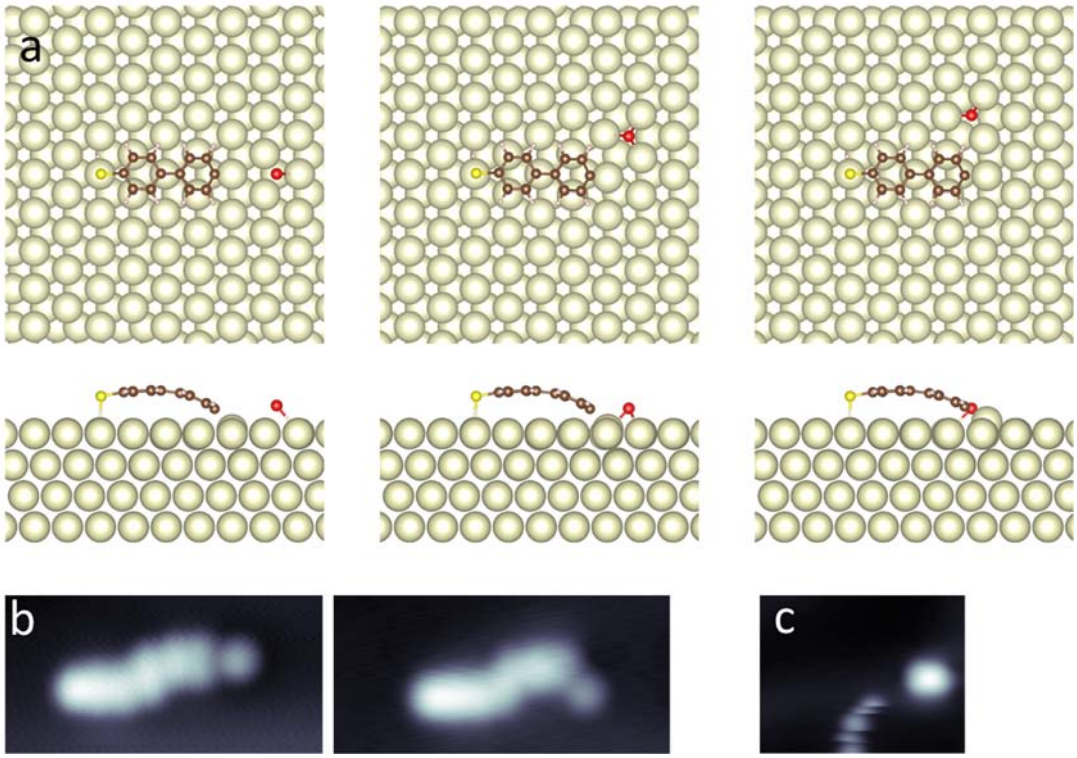

Figure ESI8. Predicted atomic positions for the dissociated Br atoms. a. Predicted atomic positions. Binding energies 1.123 eV/mol, 1.241 eV/mol, 1.260 eV/mol, for the different configurations from left to right, respectively. **b.** STM topographic images (6 nm x 3 nm) of the Br-MBP complex structures with dissociated Br atoms at different atomic positions. **c.** STM image (5.0 nm x 4.0 nm) showing the Br manipulation after its dissociation from an isolated monomeric structure.

Figure ESI8a shows the calculated equilibrium position of the dissociated Br atoms. The calculated binding energies shows that the most energetically favorable Br position after C-Br dissociation is slightly offside to the main axis of the MBP molecule, possibly favored by the molecular induced buckling of the surface. This configuration, together with the one that present the Br atom in line with the MBP main axis, has often been experimentally observed, as shown in the topographic STM images of the panel b. The dissociated halogen atoms are in weak interaction with the substrate and they can easily be manipulated away from the reaction site by the tip of the STM, as it can be observed in panel c.

ESI9. References

[1] G. Kresse, J. Furthmüller, *Comput. Mater. Sci.* **1996**, 6, 15–50

[2] G. Kresse, D. Joubert, *Phys. Rev. B* **1999**, 59, 1758–1775

[3] P. E. Blöchl, *Phys. Rev. B* **1994**, 50, 17953–17979

[4] J. P. Perdew, K. Burke, M. Ernzerhof, *Phys. Rev. Lett.* **1996**, 77, 3865–3868

[5] A. Tkatchenko, M. Scheffler, *Phys. Rev. Lett.* **2009**, 102, 073005

[6] G. Henkelman, A. Arnaldsson, H. Jónsson, *Comput. Mater. Sci.* **2006**, 36, 354−360

[7] J. Tersoff, D. R. Hamann, *Phys. Rev. B* **1985**, 31, 805–813

[8] M.-L. Bocquet, H. Lesnard, S. Monturet, N. Lorente, *In Computational Methods in Catalysis and Materials Science* (eds van Santen, R. A. & Sautet, P.) 199–219 (Wiley-VCH Verlag GmbH & Co.

[9] N. Lorente, R. Robles, STMpw (Zenodo, 2019). https://doi.org/10.5281/ZENODO.3581159.

[10] K. Momma, F. Izumi, *J. Appl. Crystallogr.* **2011**, 44, 1272–1276